Supplemental Information Inventory

1. Supplemental figures and legends

Figure S1. Levels of protein lysine succinylation and acetylation, succinate, succinyl-CoA, and acetyl-CoA in WT or *Sirt5*$^{-/-}$ animals. Related to Figure 1.

Figure S2. Venn diagram of lysine succinylated proteins and peptides identified in WT and *Sirt5*$^{-/-}$. Related to Figure 2.

Figure S3. SIRT5 and SIRT3 target sequence context heatmaps and conservation analysis. Related to Figure 3.

Figure S4. Levels of saturated acylcarnitines, unsaturated acylcarnitines, hydroxyacylcarnitines (-OH), and dicarboxylates (-DC) in WT or *Sirt5*$^{-/-}$ mouse tissues. Related to Figure 5.

Figure S5. Western blot and coomassie staining of immunoprecipitated HMGCS2 WT, K83E, K310E and K83/310E proteins. Related to Figure 7.

2. Supplemental table legends

3. Supplemental methods

4. Supplemental references

5. Supplemental tables

Dataset S1. Mass Spectrometry details for succinyllysine containing peptides isolated by affinity immunoprecipitation. Related to Figure 2 and 3.

Dataset S2. Quantification of lysine succinylated peptides by MS1 Filtering. Related to Figure 2 and 3.

Dataset S3. Succinylated proteins quantified by MS1 filtering using peptides identified from the mitochondrial lysates of WT and SIRT5 KO animals. Related to Figure 2.

Dataset S4. Mass spectrometry details for peptides identified from the mitochondrial lysate from 5 WT and 5 SIRT5 KO animals. Related to Figure 2.

Dataset S5. Conservation of succinylated lysine residues across species. Related to Figure 3.

Figure S1

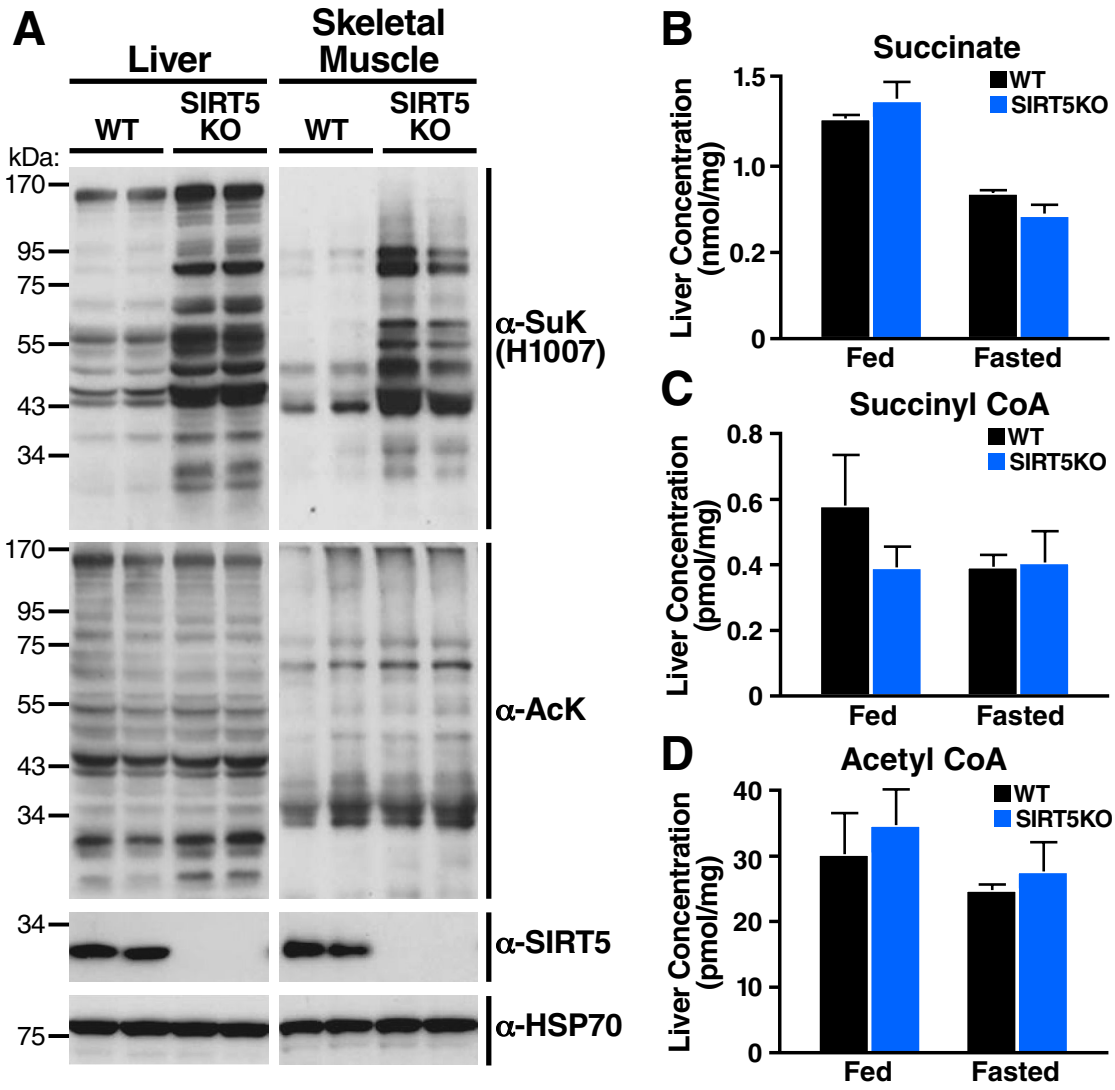
A
Liver
Skeletal Muscle
WT
SIRT5 KO
WT
SIRT5 KO
kDa:
170
95
75
55
43
34
α-SuK (H1007)
α-AcK
α-SIRT5
α-HSP70
B
Succinate
Liver Concentration (nmol/mg)
WT
SIRT5KO
Fed
Fasted
C
Succinyl CoA
Liver Concentration (pmol/mg)
D
Acetyl CoA

Figure S2

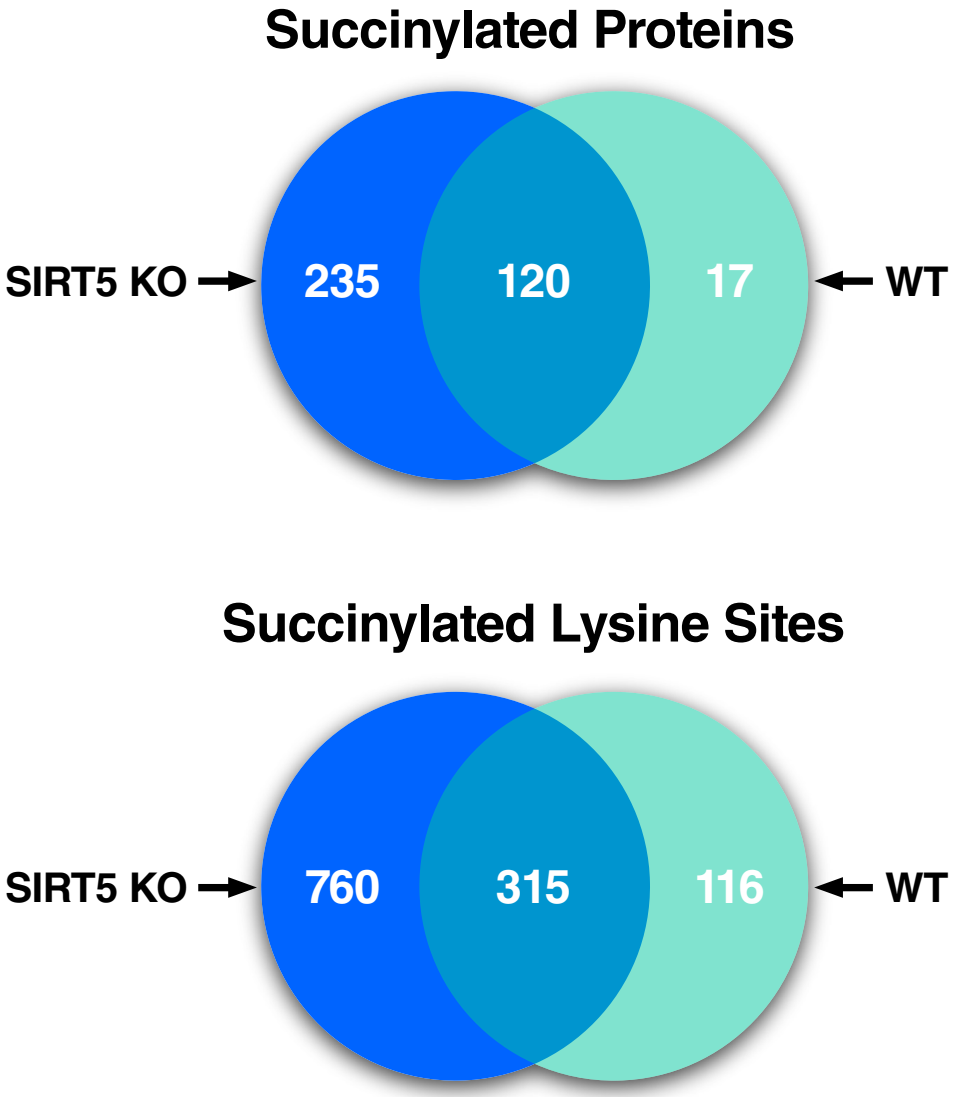
Succinylated Proteins
SIRT5 KO
235
120
17
WT
Succinylated Lysine Sites
SIRT5 KO
760
315
116
WT

Figure S3

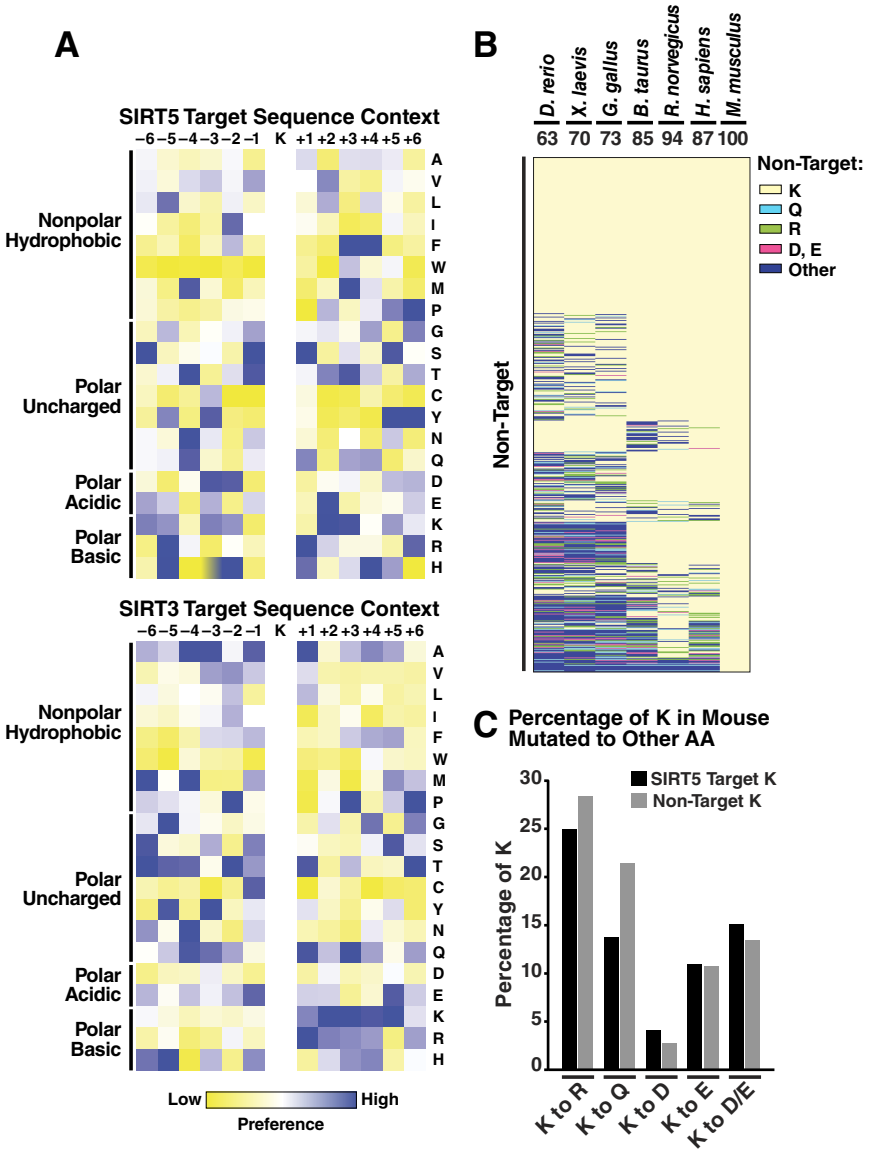
A
SIRT5 Target Sequence Context
−6 −5 −4 −3 −2 −1 K +1 +2 +3 +4 +5 +6
Nonpolar Hydrophobic
Polar Uncharged
Polar Acidic
Polar Basic
A V L I F W M P G S T C Y N Q D E K R H
SIRT3 Target Sequence Context
−6 −5 −4 −3 −2 −1 K +1 +2 +3 +4 +5 +6
Nonpolar Hydrophobic
Polar Uncharged
Polar Acidic
Polar Basic
A V L I F W M P G S T C Y N Q D E K R H
Low
High
Preference
B
D. rerio
X. laevis
G. gallus
B. taurus
R. norvegicus
H. sapiens
M. musculus
63 70 73 85 94 87 100
Non-Target
Non-Target:
K
Q
R
D, E
Other
C
Percentage of K in Mouse Mutated to Other AA
SIRT5 Target K
Non-Target K
Percentage of K
30
25
20
15
10
5
0
K to R
K to Q
K to D
K to E
K to D/E

Figure S4

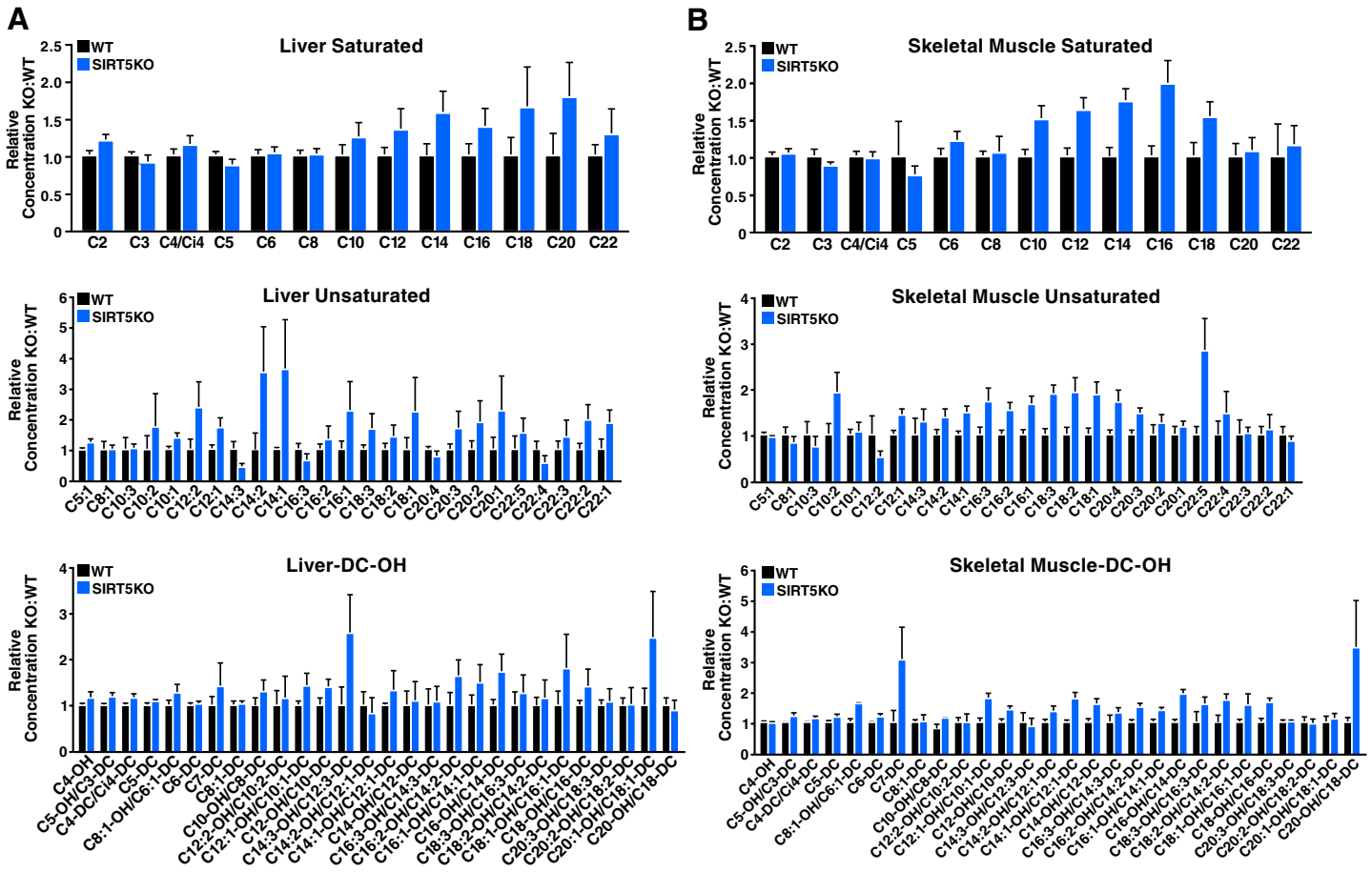
A
B
Liver Saturated
Skeletal Muscle Saturated
Liver Unsaturated
Skeletal Muscle Unsaturated
Liver-DC-OH
Skeletal Muscle-DC-OH
WT
SIRT5KO
Relative Concentration KO:WT
C2 C3 C4/Ci4 C5 C6 C8 C10 C12 C14 C16 C18 C20 C22
C5:1 C8:1 C10:3 C10:2 C10:1 C12:2 C12:1 C14:3 C14:2 C14:1 C16:3 C16:2 C16:1 C18:3 C18:2 C18:1 C20:4 C20:3 C20:2 C20:1 C22:5 C22:4 C22:3 C22:2 C22:1
C4-OH
C5-OH/C3-DC
C4-DC/Ci4-DC
C8:1-OH/C6:1-DC
C5-DC
C6-DC
C7-DC
C8:1-DC
C10-OH/C8-DC
C12:2-OH/C10:2-DC
C12:1-OH/C10:1-DC
C12-OH/C10-DC
C14:3-OH/C12:3-DC
C14:2-OH/C12:1-DC
C14:1-OH/C12:1-DC
C14-OH/C12-DC
C16:2-OH/C14:2-DC
C16:1-OH/C14:1-DC
C16-OH/C14-DC
C18:3-OH/C16:3-DC
C18:2-OH/C16:2-DC
C18:1-OH/C16:1-DC
C18-OH/C16-DC
C20:3-OH/C18:3-DC
C20:2-OH/C18:2-DC
C20:1-OH/C18:1-DC
C20-OH/C18-DC

Figure S5

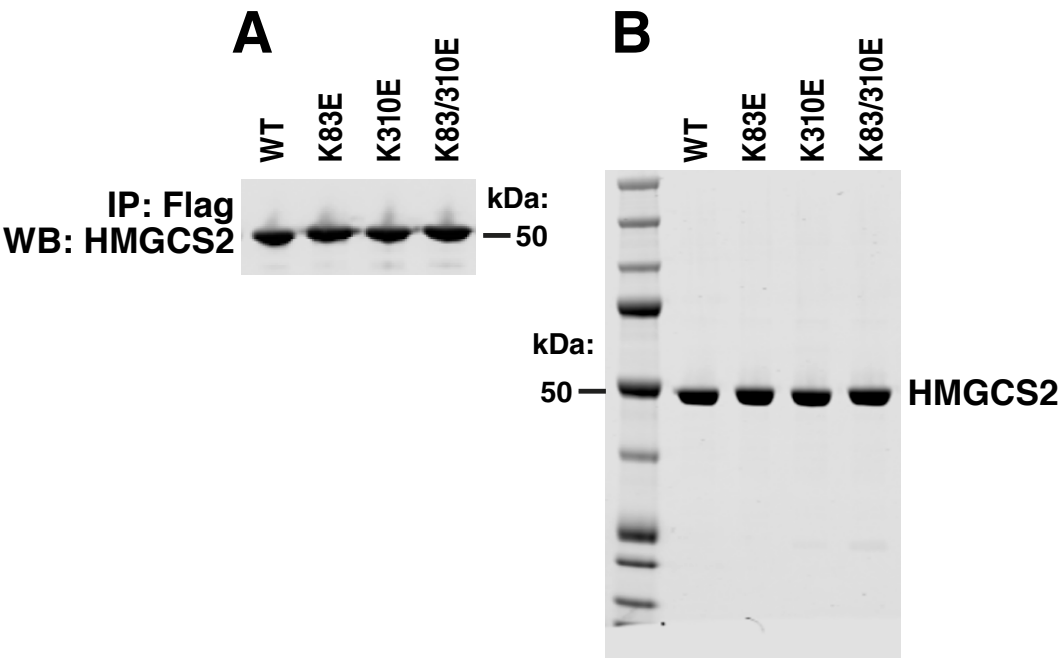
A
WT
K83E
K310E
K83/310E
IP: Flag
WB: HMGCS2
kDa:
50
B
WT
K83E
K310E
K83/310E
kDa:
50
HMGCS2

Figure S1. Levels of protein lysine succinylation and acetylation, succinate, succinyl-CoA, and acetyl-CoA in WT or *Sirt5*$^{-/-}$ animals. Related to Figure 1. (**A**) Western blot showing succinylation and acetylation of whole-tissue lysates from WT or *Sirt5*$^{-/-}$ mouse livers and skeletal muscles with the succinyl-lysine-specific antibody H1007 or an acetyl-lysine-specific antibody. Western blot for SIRT5 confirmed the absence of SIRT5 protein expression in *Sirt5*$^{-/-}$ tissues. A universally expressed mitochondrial protein HSP70 was a loading control. Levels of (**B**) succinate, (**C**) succinyl-CoA, and (**D**) acetyl-CoA in mouse livers from WT and *Sirt5*$^{-/-}$ animals under both fasted and fed conditions. Results are shown as the mean ± standard error (n=5 for succinate, n=3 for succinyl-CoA and acetyl-CoA).

Figure S2. Identification of lysine succinylated proteins and peptides. Related to Figure 2. Venn diagrams showing the overlap of identified succinylated proteins and peptides in WT and *Sirt5*$^{-/-}$ mouse liver mitochondria.

Figure S3. SIRT5 and SIRT3 target sequence context heatmaps and conservation analysis. Related to Figure 3. (**A**) The average SIRT5 KO/WT fold-change of all SuK peptides with a given amino acid at a given position was calculated. Blue represents a high fold change and strong preference for this amino acid to be associated with SIRT5 desuccinylation, while yellow represents a low fold change and less preference. Amino acids are grouped into four categories-nonpolar hydrophobic, polar uncharged, polar acidic and polar basic. SIRT3 target sequence context heatmap was also generated using our published SIRT3 study data (Rardin et al., 2013). (**B**) Heatmap depicting the conservation index of non-SIRT5 target sites across seven vertebrate species. Lysine (K), glutamine (Q), arginine (R), aspartic acid (D) or glutamic acid (E), and other amino acids are presented in different colors. (**C**) The frequency of a lysine (K) in mouse mutated to a no charge acetyl-lysine-mimic glutamine (Q), a positively charged non-acetyl-lysine-mimic arginine (R), or a

negatively charged succinyl-lysine-mimic aspartic acid (D) or glutamic acid (E) in other species was not significantly different between SIRT5 target sites and non-target sites.

Figure S4. Levels of saturated acylcarnitines, unsaturated acylcarnitines, hydroxyacylcarnitines (-OH), and dicarboxylates (-DC) in WT or *Sirt5*$^{-/-}$ mouse tissues. Related to Figure 5. Data are presented as relative concentrations in liver or skeletal muscle of WT (black bars) or *Sirt5*$^{-/-}$ mice (blue bars) (n=5). Results are shown as the mean ± standard error. Statistical analysis results are shown in Figure 5D.

Figure S5. Western blot and coomassie staining of immunoprecipitated HMGCS2 WT, K83E, K310E and K83/310E proteins. Related to Figure 7. (**A**) Plasmids for over-expressing flag tagged HMGCS2 WT or mutants were transfected into HEK293 cells. Forty eight hours post transfection, HMGCS2 WT or mutant proteins were immunoprecipitated for enzymatic activity assay. Levels of immunoprecipitated HMGCS2 WT or mutants were assessed by western blot using anti-HMGCS2 antibody. (**B**) Coomassie staining was also performed showing the purity and equal amounts of immunoprecipitated HMGCS2 WT or mutants.

Dataset S1. Mass Spectrometry details for succinyllysine containing peptides isolated by affinity immunoprecipitation. Related to Figure 2 and 3.

Dataset S2. Quantification of lysine succinylated peptides by MS1 Filtering. Related to Figure 2 and 3. Lysine succinylated peptides identified by HPLC-MS/MS and quantified by MS1 Filtering. Multiple peptides may have been identified, however representative high-confidence peptides were selected based on having a tryptic cleavage at arginine or a non-succinylated lysine, most abundant charge state, and/or lacking any secondary modifications when available.

Dataset S3. Succinylated proteins quantified by MS1 filtering using peptides identified from the mitochondrial lysates of WT and SIRT5 KO animals. Related to Figure 2. Peptides were quantified by MS1 Filtering and a peptide ratio of KO:WT was generated. The average of those peptide ratios were used to generate a protein ratio KO:WT. 203 succinylated proteins were quantified along with an additional 33 proteins that were not identified as being succinylated.

Dataset S4. Mass spectrometry details for peptides identified from the mitochondrial lysate from 5 WT and 5 SIRT5 KO animals. Related to Figure 2.

Dataset S5. Conservation of succinylated lysine residues across species. Related to Figure 3.

Supplementary methods

Materials. HPLC solvents, including acetonitrile and water, were obtained from Burdick & Jackson (Muskegon, MI). Reagents for protein chemistry, including iodoacetamide, dithiothreitol (DTT), ammonium bicarbonate, formic acid, trifluoroacetic acid, trichostatin A, dodecyl-maltoside, urea, nicotinamide, and bovine serum albumin (BSA), were purchased from Sigma Aldrich (St. Louis, MO). Succinylated synthetic peptide containing a stable isotope labeled arginine residue (ADIAESQVNK[Succinyl]LR[$^{13}C_6{}^{15}N_4$]) was obtained from Thermo Fisher Scientific at >95% purity. Tris(2-carboxyethyl)phosphine (TCEP) and protein A/G magnetic beads were purchased from Thermo Scientific (Rockford, IL), and HLB Oasis SPE cartridges were purchased from Waters (Milford, MA). Proteomics grade trypsin was from Promega (Madison WI). Trypsin-predigested β-galactosidase (a quality control standard) was purchased from AB SCIEX (Foster City, CA).

Mass spectrometry (MS) and chromatographic parameters. The autosampler was operated in full injection mode filling a 3-µl loop with 3 µl of analyte for sample delivery. Briefly, after injection, peptide mixtures were transferred onto the analytical C18-nanocapillary LC column (C18 Acclaim PepMap100, 75 µm I.D. x 15 cm, 3-µm particle size, 100Å pore size, Dionex, Sunnyvale, CA) and eluted at a flow rate of 300 nL/min with the following gradient: at 5% solvent B in A (from 0–13 min), 5–35% solvent B in A (from 13–58min), 35–80% solvent B in A (from 58–63 min), 80% solvent B in A (from 63–66 min), and 80–5% solvent B in A (from 66–68 min), with a total runtime of 90 min, including mobile phase equilibration. Solvents were prepared as follows, mobile phase A: 2% acetonitrile/98% of 0.1% formic acid (v/v) in water, and mobile phase B: 98% acetonitrile/2% of 0.1% formic acid (v/v) in water. Mass spectra and tandem mass spectra were recorded in positive-ion and "high-sensitivity" mode with a resolution of ~35,000 full-width half-maximum in MS1 and 15,000 in MS2. The nanospray needle voltage was typically 2,400 V in HPLC-MS mode. After acquisition of two samples, TOF MS spectra and TOF MS/MS spectra were automatically calibrated during dynamic LC-MS & MS/MS autocalibration acquisitions injecting 25 fmol of a β-galactosidase tryptic digest. For collision-induced dissociation tandem mass spectrometry (CID-MS/MS), the mass window for precursor ion selection of the quadrupole mass analyzer was set to ± 1 *m/z*. The precursor ions were fragmented in a collision cell by nitrogen as the collision gas. Advanced information dependent acquisition (IDA) was used for MS/MS collection on the TripleTOF 5600 to obtain MS/MS spectra for the 20 most abundant parent ions after each survey MS1 scan (allowing typically for 50 msec acquisition time per each MS/MS). Dynamic exclusion features were based on value M not *m/z* and were set to an exclusion mass width of 50 mDa and an exclusion duration of 15–20 sec. MS/MS spectra for all identified peptides may be viewed using Panorama at the following location http://proteome.gs.washington.edu/software/panorama/sirt5_succinylome.html. The raw mass

spectrometry data files have been deposited using an FTP site hosted at the Buck Institute, ftp://mattr:publication@sftp.buckinstitute.org:248/.

Affinity purification of lysine-succinylated peptides. The polyclonal anti-succinyl lysine antibodies (Cell Signaling Technology, H1006 and H1007) were immobilized on protein A/B magnetic beads (4°C, 2 h). Succinyllysine peptide standard (150 fmol of ADIAESQVNsuKL**R**[$^{13}C_6{}^{15}N_4$]) was added to the digested peptides from the above mitochondrial protein lysate and incubated overnight at 4°C at a 1:20 antibody:peptide ratio (wt/wt). Beads were washed three times in NET buffer, and the peptides eluted by washing three times in 1% trifluoroacetic acid/40% acetonitrile. Peptides are concentrated to near dryness by vacuum centrifugation and resuspended in equal amounts of 0.1% formic acid/1% acetonitrile. The succinyllysine peptide enrichments were subsequently desalted using C-18 zip-tips. After evaporation of organic solvents, samples were suspended in 0.1% formic acid/1% acetonitrile and analyzed by LC-MS/MS on the TripleTOF 5600. A solution-only “blank” or auto-calibration was examined between sample acquisitions to prevent carry over that would affect downstream quantitative analysis.

Bioinformatic database searches. Search parameters in Mascot for succinylated peptides were as follows. Trypsin digestion with four missed cleavages accounted for the inability of trypsin to cleave at succinylated lysine residues. Trypsin specificity was set to C-terminal cleavage at lysine and arginine. Variable modifications included lysine succinylation, methionine oxidation, conversion of glutamine to pyroglutamic acid, and deamidation of asparagine. Carbamidomethyl cysteine was set as a fixed modification. Precursor ion and fragment ion mass tolerances were set to 20 ppm and 0.2 Da, respectively. Peptides with an expectation value below the 1% false discovery rate (FDR) were chosen for further data processing.

The following sample parameters were used in Protein Pilot: trypsin digestion, cysteine alkylation set to iodoacetamide, urea denaturation, and succinylation emphasis. Processing parameters were set to "biological modification," and a thorough ID search effort was used. A local FDR of 1% was chosen using the Protein Pilot false discovery rate analysis tool (PSPEP) algorithm (Shilov et al., 2007). All mass spectral details for succinylated peptides are available in Dataset S1. For non-succinylated peptide searches the succinylation emphasis was not used and a peptide confidence value of 95 was chosen, mass spectral details for non-enriched peptides are available in Dataset S4.

Skyline MS1 Filtering tool algorithm and data analysis. Skyline is an open-source software project and can be freely installed. Additional details and tutorials for creating spectral libraries and MS1 filtering can be viewed on the Skyline website (http://proteome.gs.washington.edu/software/skyline). Spectral libraries were generated in Skyline with the BiblioSpec algorithm (Frewen and MacCoss, 2007) from database searches of the raw data files as described (Schilling et al., 2012). Raw files were directly imported into Skyline in their native file format, which Skyline achieves using the ProteoWizard data access library (Kessner et al., 2008). After data import, graphical displays of chromatographic traces for the top three isotopic peaks were manually inspected for proper peak picking of MS1 filtered peptides. All quantifications performed in this study were done on the peptide level, using a peptide centric approach. Only the most abundant isotope for each peptide was used for quantitation. The following data extraction peptide areas were normalized to the spiked in succinyllysine peptide standard (ADIAESQVNsuKL**R** with the most abundant precursor at *m/z* 727.38 $^{++}$; where SuK is N-succinyllysine and R= $^{13}C_6{}^{15}N_4$-Arg) and multiplied by a normalization factor $1e^7$ to ensure all values were greater than 1. The normalized peptide area was then averaged across all WT or *Sirt5*$^{-/-}$ acquisitions, and a ratio generated (KO:WT). *P*-values were calculated using a two-tailed, unpaired Student's t-test. For protein quantification peptides identified from the mitochondrial lysate

(Dataset S3) that corresponded to succinylated proteins from our enrichment analysis were analyzed by MS1 Filtering. Protein expression was determined by averaging the individual peptide KO:WT ratios. All details for peptide quantitation by MS1 Filtering are provided in Dataset S2 and S3.

Sample preparation of mouse liver mitochondrial for MS analysis. 1.5 mg of mitochondrial protein per mouse was denatured with 1% dodecyl-maltoside and 10 M urea per process replicate. Samples were then diluted 1:10, reduced with 4.5 mM TCEP (37C for 1 h), alkylated with 10 mM iodoacetamide (30 min at RT in the dark), and incubated overnight at 37 degree with sequencing grade trypsin added at a 1:50 enzyme:substrate ratio (wt/wt). Samples were then acidified with formic acid and desalted using HLB Oasis SPE cartridges. Samples were eluted, concentrated to near dryness by vacuum centrifugation, and resuspended in NET buffer (50 mM Tris-HCl, pH 8.0, 100 mM NaCl, 1 mM EDTA). 15 g of the protein digest from each sample was desalted using C-18 zip-tips for total peptide analysis of samples by MS1 Filtering, while the remaining protein digest was used for affinity purification of lysine-succinylated peptides.

Western blot. Western blot was performed to test the specificity of newly developed acyl-lysine antibodies with BSA carrying distinct acylation modifications. The levels of global lysine succinylation, and acetylation in whole-cell lysates of liver, skeletal muscle, primary hepatocytes or MEFs of wild-type and *Sirt5*$^{-/-}$ mice as well as in liver subcellular fractions were also examined by western blot. Antibodies used are listed as follows: α-succinyl-lysine (Cell Signaling Technology, H1006, H1007), α-acetyl-lysine (Cell Signaling Technology, #9814), α-butyryl/propionyl-lysine (Cell Signaling Technology, BL11898), α-HSP70 (Piece, MA3-028), anti-tubulin (Sigma-Aldrich, St. Louis, MO), anti-VDAC (Cell Signaling Technology, Danvers, MA), anti-HMGCS2 (Santa Cruz Biotechnology, Dallas, TX), anti-Flag M2 (Sigma-Aldrich, St. Louis, MO), anti-HA (Roche Diagnostics, Indianapolis, IN).

Antibodies for detecting murine SIRT5 were raised in rabbits using the C-terminal peptide GPCGKTLPEALAPHETERT (Covance Research Products, Inc.).

Tissue subcellular fractionation. The subcellular extraction was prepared in accordance with previous reports (Cox and Emili, 2006). Briefly, liver tissues were homogenized in ice-cold 250-STMDPS buffer (50 mM Tris-HCl, pH 7.4, 250 mM sucrose, 5 mM $MgCl_2$, 1 mM DTT, 1 mM PMSF, 25 μg/ml spermine and 25 μg/ml spermidine) with a Dounce homogenizer. The extract was centrifuged at 800 *g* for 15 min to remove nuclei. The supernatant was again centrifuged at 6000 *g* for 15 min to spin down mitochondria (Pellet II). Residual supernatants were centrifuged at 100,000 g for 60 min to obtain pure cytosolic fraction. Pellet II was resuspended in hypotonic lysis buffer (10 mM HEPES, pH 7.9, 1 mM DTT, plus the Halt inhibitor cocktail; ThermoScientific) and incubated on ice for 30 min. The suspension was sonicated to lyse mitochondria. Protein concentrations were determined for the nuclear fraction and the mitochondrial lysate using the standard BCA assay following the manufacturer's protocol (ThermoScientific). The purity of the extracted nuclear fraction was validated by Western blot.

Mouse hepatocyte isolation. Hepatocytes were isolated at UCSF Liver Center according to described methods (Seglen, 1972). Briefly, the liver of wild-type or *Sirt5*$^{-/-}$ mice was perfused in-situ with a calcium-chelating solution, followed by a collagenase buffer. Upon digestion, the liver was removed and minced and filtered to remove any remaining liver tissue. The cell suspension was centrifuged two times at 90 g, and the supernatant discarded. The pellet was re-suspended and underlain with 50% Percoll and spun at 200 g. After two more washes, cell pellets were resuspended and viable cells were counted. 10^6 cells were seeded in a 60-mm dish and cultured in M199 medium with 10% FBS.

Overlap Analysis of SIRT3 with SIRT5. For combining SIRT3-acetylation dataset with the current SIRT5-succinylation dataset, we aligned each original modified sequence from the SIRT3 dataset with the downloaded full UniProt sequence (same database file used for aligning SIRT5 dataset). We then joined the datasets on the unique combination of UniProt accession and lysine position within that UniProt sequence.

Generation and characterization of succinyl-lysine-specific antibodies. Succinyl lysine antibodies were generated by immunizing New Zealand White rabbits using succinylated KLH (keyhole limpet hemocyanin) at Cell Signaling Technology (Danvers, MA). Rabbit serum was screened by ELISA to test reactivity with degenerate succinylated peptide library. The reactive rabbit serum was then purified over peptide affinity column. Purified antibodies were tested against acetyl-BSA, propionyl-BSA, butyryl-BSA, and succinyl-BSA to confirm the specificity.

Animals. Animal studies were performed according to protocols approved by IACUC (the Institutional Animal Care and Use Committee). Wild-type and *Sirt5*$^{-/-}$ male mice on 129 background were maintained on a standard chow diet (5053 PicoLab diet, Purina) until they were sacrificed for experiments.

Generation of context heatmaps. To create the sequence context heatmap, we calculated the mean ratio (KO/WT) for all succinylpeptides with a given amino acid at each context position (-6 to +6) among the entire dataset. Colors gradients reach the maximum value at +/- 2 standard deviations from the overall mean ratio. Similarly, SIRT3 target sequence context heatmap was generated using the data from our previous study of lysine acetylation in liver mitochondria from WT and *Sirt3*$^{-/-}$ mice (Rardin et al., 2013).

Deuterium-palmitate oxidation assay. Mouse liver hepatocytes were incubated with either control medium or glucose-deprived medium supplied with 200 µM [^{2}H31]-palmitate conjugated to fatty acid–free BSA. 1 mM stock of [^{2}H31]-palmitate-BSA was prepared according to the protocol developed at Seahorse Bioscience. Plates with experimental medium but no cells were negative controls. The specificity of this assay was tested by co-incubation with 100 µM Etomoxir (fatty acid oxidation inhibitor). At 24 or 48 hrs later, the culture medium was collected, and the water was isolated by micro-distillation at 45°C in a refrigerated environment (4^{o}C). The deuterium content of the distillates was determined using a ThermoFinnigan High Temperature Conversion/Elemental Analyzer coupled with a ThermoFinnigan MAT 253 isotope ratio-mass spectrometer via a Conflo-III Interface. The deuterium isotope abundance was calculated in δ 2H values relative to the international Vienna Standard Mean Ocean Water, and then the rate of palmitate oxidation was calculated and expressed as µmoles of palmitate oxidized per 10^{6} cells from the production of deuterium labeled water. *P*-values were calculated using a two-tailed, unpaired Student's t-test.

Tritium-palmitate oxidation assay. SV40-transformed wild-type and *Sirt5*$^{-/-}$ mouse embryonic fibroblasts were plated in 24-well plates and grown to approximately 75% confluency. Medium was replaced with 300 µl of low glucose (1 g/L) DMEM containing 10% FBS, 1 mM L-carnitine, and 100 µM [9,10-^{3}H]-palmitate (Perkin Elmer) conjugated to fatty acid–free BSA. Four wells of cells on each plate were "mock-treated," receiving no palmitate-BSA, and were later lysed for protein assay. Negative controls were wells with experimental medium but no cells. The plates were returned to the cell-culture incubator for either 3 or 24 hours. At the end of the incubation, the experimental medium, including from negative control wells, was removed and subjected to organic extraction as described (Bligh and Dyer, 1959). The aqueous layer, containing $^{3}H_2O$ released by fatty acid β-oxidation, was

used for scintillation counting. The rate of palmitate oxidation is expressed as nmoles of palmitate oxidized per mg cellular protein. *P*-values were calculated using a two-tailed, unpaired Student's t-test.

Metabolomics from mouse tissues. Measurement of tissue acylcarnitine levels were performed at the Duke University Metabolomics Core (Stedman Center). Mouse liver or skeletal muscle was collected from fed wild-type or *Sirt5*$^{-/-}$ male mice at 16 weeks of age and snap-frozen in liquid nitrogen. Frozen tissues were first ground into powders in liquid nitrogen, and proteins were precipitated with methanol. Supernatants were dried, esterified with hot, acidic methanol (acylcarnitines), and analyzed by tandem mass spectrometry (Quattro Micro, Waters Corporation) (Hirschey et al., 2010; Jensen et al., 2006). The concentration levels for each acylcarnitine were scaled by dividing by the average concentration of that acylcarnitine in WT mice. This scales the WT level to an average value of one for each acylcarnitine, and the scaled KO level can be interpreted as a relative concentration in KO vs. WT. This normalization was performed separately in each tissue type.

Statistical analysis of mouse tissue acylcarnitines. Preliminary graphical analyses suggested similarities between relative concentrations (KO:WT) in liver and skeletal muscle, so data from these two tissues were analyzed using a single combined model. For each chain length category, the relative concentration of acylcarnitines in KO vs. WT mice was estimated using a Bayesian model. The model included random effects for each mouse and for each tissue x saturation x modification triplet. We fit the model with the Markov chain Monte Carlo algorithm using the statistical programming language R.

Let y_{atig} denote the relative concentration of acylcarnitine *a* from tissue *t* from mouse *i* from genotype *g*. Furthermore, for acylcarnitine *a*, let *c*[*a*] denote its chain length, *s*[*a*] denote its saturation, and *m*[*a*] denote its modification.

We specified the following likelihood for each relative concentration value: $y_{a,t,i,g} = 1 + \beta_{g,c[a]} + \alpha_{g,t,c[a],s[a],m[a]} + \gamma_i + \varepsilon_{a,t,i,g}$.

- A fixed intercept of one is used to capture the scaling of each concentration by its tissue-specific WT average.
- The primary goal of inference was to describe the effect of genotype for each chain length, so for each chain length c, we let $\beta_{g,c[a]}$ capture the chain-length specific genotype effect. We set $\beta_{g,c[a]}$ to zero for measurements from WT mice. Each of the three β's was given an independent flat prior.
- Since tissue type, saturation, and modification were of secondary interest, we created strata to describe the tissue × saturation × modification triplets for each chain length. Exchangeable random effects for these strata were given by α. We set $\alpha_{g,t,c[a],s[a],m[a]}$ to zero for measurements from WT mice. The prior for the α's was $\mathcal{N}(0, \sigma_\alpha^2)$.
- Mouse-specific random effects were given by γ, with $\gamma \sim \mathcal{N}(0, \sigma_\gamma^2)$.
- Residual variability due to measurement error and other unmeasured factors was captured by $\varepsilon \sim \mathcal{N}(0, \sigma_\varepsilon^2)$.
- For each of the three variance components, we use a flat prior on the standard deviation scale (Gelman, 2006): $P(\sigma) \propto 1$.

We fit the model with the Markov chain Monte Carlo (MCMC) algorithm using the statistical programming language R (Team, 2012). The 95% credible intervals represent the 2.5–97.5 percentiles of the posterior distribution. We calculated p-values by inverting these credible intervals (Altman, 2011). We note that multiple comparisons corrections were not needed since the priors in this Bayesian model result in "partial pooling" (Gelman, 2012). Tissue-specific results were obtained

by averaging over the saturation × modification strata for each tissue type.

We started three MCMC chains from over-dispersed initial values. After 25,000 iterations of burn-in, we obtained 25,000 additional samples from each chain. Convergence was achieved, with all chains having Gelman Rubin statistics (Gelman, 1992) of 1. We combined the three chains and thinned to obtain 5000 iterations with which to do inference. Mixing sufficed to yield >4000 effectively independent samples (Plummer, 2006) from each chain.

Liver β-hydroxybutyrylcarnitines (C4-OH) concentrations in fed or fasted wild-type or *Sirt5*$^{-/-}$ mice are shown as mean ± standard error. *P*-values were calculated by unpaired *t* test.

Ketone Body Measurement. The concentration of ketone body in the plasma of mice was determined by using a Stanbio β-hydroxybutyrate LiquiColor endpoint test kit, according to the manufacturer's instructions. Briefly, 6 µl of standards or plasma samples were added to 251 µl of R1 (warmed up at 37°C) and baseline was immediately measured spectrophotometrically at 505nm. Then 38 µl of R2 was added and incubated at 37 degree for 5 mins. Endpoint was measured again at 505nm. The concentration of plasma β-hydroxybutyrate was calculated according to standard curve. Results are shown as mean ± standard error. *P*-values were calculated by unpaired *t* test.

Construction of SIRT5 shRNA. A modified version of the pSicoR lentiviral vector (Ventura et al., 2004) that encodes the mCherry reporter gene driven by an EF-1α promoter (pSicoRMS) was used to carry specific shRNAs. ShRNAs targeting SIRT5 (SIRT5 #1: GTCTCCAGATTCAAATATA, SIRT5 #3: GAAAGAAATTACAGTATAT) were cloned into pSicoRMS. Knockdown efficiency was confirmed by western blot of SIRT5 protein levels.

Immunoprecipitation. Cells were lysed on ice in RIPA buffer (50mM Tris, 150mM NaCl, 1% triton-X100, 0.5% sodium deoxycholate, and 0.1% SDS) with Halt protease and phosphatase inhibitor cocktail (ThermoScientific). Flag-tagged proteins were immunoprecipitated, washed in RIPA buffer

four times, and eluted with 0.1 mg/ml Flag peptide. For immunoprecipitation of endogenous HMGCS2, anti-HMGCS2 polyclonal antibody (Sigma-Aldrich, St. Louis, MO) was used followed by precipitation with goat anti-chicken IgY antibody beads (ProSci, Poway, CA).

***In vitro* HMGCS2 Activity Assay**. Flag-HMGCS2 proteins were immunoprecipitated from HEK293 cells and HMGCS2 activity was measured as previously described (Andrew Skaff and Miziorko, 2010; Shimazu et al., 2010). Briefly, conversion of acetyl-CoA and acetoacetyl-CoA to 3-hydroxy-3-methylglutaryl-CoA was measured by detection of free CoA-SH by 5,5'-dithiobis-(2-nitrobenzoic acid) or DTNB. Assay buffer contained 70 mM Tris-Cl (pH 8.0), 130 μM DTNB (A412 nm = 13.6 mM^{-1}), 50-1600 μM acetyl-CoA, 10 μM acetoacetyl-CoA, and 1 μg of enzyme in a final volume of 200 μL. To determine Km and Vmax data were fitted by non-linear regression to the Michaelis-Menten equation (R2 > 0.98). Each data point is the average of three separate measurements. Curves are representative of two independent experiments.

Supplemental references

Altman, D.G., & Bland, J. M. (2011). How to obtain the P value from a confidence interval. BMJ *343*.

Andrew Skaff, D., and Miziorko, H.M. (2010). A visible wavelength spectrophotometric assay suitable for high-throughput screening of 3-hydroxy-3-methylglutaryl-CoA synthase. Anal Biochem *396*, 96-102.

Bligh, E.G., and Dyer, W.J. (1959). A rapid method of total lipid extraction and purification. Can J Biochem Physiol *37*, 911-917.

Cox, B., and Emili, A. (2006). Tissue subcellular fractionation and protein extraction for use in mass-spectrometry-based proteomics. Nat Protoc *1*, 1872-1878.

Frewen, B., and MacCoss, M.J. (2007). Using BiblioSpec for creating and searching tandem MS peptide libraries. Curr Protoc Bioinformatics *Chapter 13*, Unit 13 17.

Gelman, A. (2006). Prior distributions for variance parameters in hierarchical models. Bayesian analysis *1*, 515-534.

Gelman, A., & Rubin, D. B. (1992). Inference from iterative simulation using multiple sequences. Statistical Science, 457-472.

Gelman, A., Hill, J., & Yajima, M. (2012). Why we (usually) don't have to worry about multiple comparisons. Journal of Research on Educational Effectiveness *5*, 189-211.

Hirschey, M.D., Shimazu, T., Goetzman, E., Jing, E., Schwer, B., Lombard, D.B., Grueter, C.A., Harris, C., Biddinger, S., Ilkayeva, O.R.*, et al.* (2010). SIRT3 regulates mitochondrial fatty-acid oxidation by reversible enzyme deacetylation. Nature *464*, 121-125.
Jensen, M.V., Joseph, J.W., Ilkayeva, O., Burgess, S., Lu, D., Ronnebaum, S.M., Odegaard, M., Becker, T.C., Sherry, A.D., and Newgard, C.B. (2006). Compensatory responses to pyruvate carboxylase suppression in islet beta-cells. Preservation of glucose-stimulated insulin secretion. J Biol Chem *281*, 22342-22351.
Kessner, D., Chambers, M., Burke, R., Agus, D., and Mallick, P. (2008). ProteoWizard: open source software for rapid proteomics tools development. Bioinformatics *24*, 2534-2536.
Plummer, M., Best, N., Cowles, K., & Vines, K. (2006). CODA: Convergence Diagnosis and Output Analysis for MCMC. R News *6*, 7-11.
Rardin, M.J., Newman, J.C., Held, J.M., Cusack, M.P., Sorensen, D.J., Li, B., Schilling, B., Mooney, S.D., Kahn, C.R., Verdin, E.*, et al.* (2013). Label-free quantitative proteomics of the lysine acetylome in mitochondria identifies substrates of SIRT3 in metabolic pathways. Proc Natl Acad Sci U S A *110*, 6601-6606.
Schilling, B., Rardin, M.J., MacLean, B.X., Zawadzka, A.M., Frewen, B.E., Cusack, M.P., Sorensen, D.J., Bereman, M.S., Jing, E., Wu, C.C.*, et al.* (2012). Platform-independent and label-free quantitation of proteomic data using MS1 extracted ion chromatograms in skyline: application to protein acetylation and phosphorylation. Mol Cell Proteomics *11*, 202-214.
Seglen, P.O. (1972). Preparation of rat liver cells. I. Effect of Ca 2+ on enzymatic dispersion of isolated, perfused liver. Exp Cell Res *74*, 450-454.
Shilov, I.V., Seymour, S.L., Patel, A.A., Loboda, A., Tang, W.H., Keating, S.P., Hunter, C.L., Nuwaysir, L.M., and Schaeffer, D.A. (2007). The Paragon Algorithm, a next generation search engine that uses sequence temperature values and feature probabilities to identify peptides from tandem mass spectra. Mol Cell Proteomics *6*, 1638-1655.
Shimazu, T., Hirschey, M.D., Hua, L., Dittenhafer-Reed, K.E., Schwer, B., Lombard, D.B., Li, Y., Bunkenborg, J., Alt, F.W., Denu, J.M.*, et al.* (2010). SIRT3 deacetylates mitochondrial 3-hydroxy-3-methylglutaryl CoA synthase 2 and regulates ketone body production. Cell Metab *12*, 654-661.
Team, R.D.C. (2012). R: A language and environment for statistical computing (Vienna, Australia, R. Foundation for Statistical Computing).
Ventura, A., Meissner, A., Dillon, C.P., McManus, M., Sharp, P.A., Van Parijs, L., Jaenisch, R., and Jacks, T. (2004). Cre-lox-regulated conditional RNA interference from transgenes. Proc Natl Acad Sci U S A *101*, 10380-10385.